PROCEEDINGS OF SCIENCE

The Detection of *Fermi* AGN above 100 GeV using Clustering Analysis

Thomas Armstrong*
Dept. of Physics and Centre for Advanced Instrumentation, Durham University
E-mail: thomas.armstrong@durham.ac.uk

Anthony M. Brown
Dept. of Physics and Centre for Advanced Instrumentation, Durham University
E-mail: anthony.brown@durham.ac.uk

Paula. M. Chadwick
Dept. of Physics and Centre for Advanced Instrumentation, Durham University
E-mail: p.m.chadwick@durham.ac.uk

S. J. Nolan
Dept. of Physics and Centre for Advanced Instrumentation, Durham University
E-mail: s.j.nolan@durham.ac.uk

The 6-year Fermi dataset contains some 8000 extragalactic events with E >100GeV. To search for the sources of these events, we applied a clustering algorithem (DBSCAN), using a search radius based on the *Fermi*-LAT point spread function, to events from >10 degrees above and below the Galactic plane. This analysis revealed 49 significant clusters. Of these, 21 correspond to known Very High Energy (VHE) emitting Active Galactic Nuclei (AGN) in the TeVCat catalogue and 9 represent new VHE sources - 6 BL Lacs, one blazar of unknown type and two unidentified sources. These objects are compared with the known VHE AGN population and the prospects for follow-up observations with ground based γ-ray observatories are considered.

The 34th International Cosmic Ray Conference,
30 July- 6 August, 2015
The Hague, The Netherlands

*Speaker.

PoS(ICRC2015)783

1. Introduction

Since its launch in 2008, the *Fermi* space-based γ-ray telescope has spent $\sim 95\%$ of its time in *all-sky-survey* mode, in which the Large Area Telescope (LAT) scans the entire sky every two orbits, or approximately every 3 hours [5]. Information on location, time and energy is recorded for each event detected, resulting in a large, multi-dimensional database which provides us with a wealth of information about the γ-ray sky.

The *Fermi* third point source catalogue (3FGL [11]), released in January 2015, is the main source of information for gamma-ray sources in the 0.1 to 100 GeV energy range. The method used to create this data set relied on wavelet-based algorithms (see [11]) and minimum spanning trees (MST, [8]), followed up by a full likelihood analysis. However there has been a substantial amount of work on clustering analysis for classifying large data sets into meaningful subsets. It is therefore likely that these methods are worthy of investigation as potential source-finding algorithms for the LAT data set.

Alongside the MST clustering performed in the source detection for the 3FGL, investigation into clustering performance for *Fermi* was carried out in [15] using the density-based clustering algorithm DBSCAN (Density-Based Spatial Clustering of Applications with Noise; [10]). By applying the cluster analysis to simulated *Fermi*-LAT data, Tramacere & Vecchio were able to show the statistical robustness of the code's ability to identify potential sources in noisy regions.

In this paper we have chosen to apply a cluster analysis to all $E_\gamma \geqslant 100$ GeV photons with $\mid b \mid > 10^\circ$. Firstly, since the extragalactic diffuse background has a spectral index of 2.41, we reduce complications due to background noise which mainly affect lower energies [2]. Secondly, as the computational complexity of DBSCAN runs as $O(n^2)$[1], by using only the high-energy events we are able to run a full, unbiased and model-independent clustering analysis of the whole sky without using a large amount of computing time. Finally, the possibility of increasing the known VHE γ-ray population of active galactic nuclei (AGN), particularly in the light of framing the scientific priorities for the forthcoming Cherenkov Telescope Array [4, 14].

This paper is organised as follows. In Section 2, we discuss the use of clustering, the chosen method and its application to *Fermi*-LAT VHE events. The clusters are verified using *Fermi* tools in Section 3 and the results, along with a preliminary analysis of the global properties of the detected sources, are discussed in Section 4.

2. Clustering Algorithms

DBSCAN: The base version of DBSCAN requires two input parameters, *MinPts*, the smallest number of events we would consider to constitute a cluster within a circle of radius *EPS*, which is the second parameter. The main concept of DBSCAN centres around the idea of *core samples* in areas of higher density. A core sample is defined as a point, p, which satisfies the condition $N_{EPS}(p) \geqslant MinPts$. That is, p is a core point if the number of events within its *EPS*-Neighbourhood is equal to or greater than that given by the *MinPts* parameter. The code we used is built on the Scikit-Learn python library in which the clusters are computed as follows:

[1] It is possible to improve the speed up to $O(n\ logn)$ by pre-computing the *EPS*-neighbourhoods (see Section 2)

1. for each point p in a set of objects D, the number of points within the *EPS*-Neighbourhood ($N_{EPS}(p)$) is found;
2. if the core sample condition $N_{EPS}(p) \geqslant MinPts$ is satisfied, then p is a core point and is added to the cluster C;
3. if a point q within the *EPS*-Neighbourhood of the core point p also satisfies the core sample condition then p and q are *density-connected* and q is added to C. If not, it is classified as a *border point* or *density-reachable*;
4. step (3) is repeated for every candidate core point for C;
5. the algorithm moves to a new, unprocessed, core point and returns to step (2).

One of the difficulties of using DBSCAN is that the initial choice of *EPS* and *MinPts* strongly affect the outcome of the clustering algorithm. However, [15] performed a statistical analysis using DBSCAN on simulated data to determine optimum choices for *EPS* and *MinPts* and to test the robustness of the algorithm. It was shown that *EPS* can be related to the point spread function (PSF) of the LAT detector. In the case of our application to clustering above 100 GeV, as the pass 7 *Fermi*-LAT response functions give a PSF of $\sim$0.1° at 100 GeV for a 68% containment radius and 0.5° for 95% [3], we investigated a range between these values in [1] and arrived at a optimum of 0.4° in order to maximise source detection.

A second limitation of DBSCAN is its inability to deal with a spatially non-uniform background. In these cases, the intrinsic cluster structure may be masked by a non-ideal global set of parameters. For our application of clustering off-plane at energies greater than 100 GeV, the variation in the diffuse background is greatly reduced to the point where it can be considered negligible.

Clustering of VHE Gamma-Ray Events The VHE domain provides a good testbed for the validation of DBSCAN. With its long exposure time and full sky coverage, *Fermi* gives us access to the deepest extragalactic scan presently available in the 100-300 GeV energy range. Indeed, recent work took advantage of *Fermi*-LAT's deep exposure to discover two new VHE-bright AGN [6, 7]. It is important to note, however, that these studies only searched for VHE emission around bright, spectrally hard, *Fermi*-LAT detected BL Lac objects. Given the relatively small number known of VHE gamma-ray objects, it is important that we investigate statistical methods in the context of a model-independent search, which could lead to greater understanding of VHE populations.

For our data set, we took all *Fermi*-LAT events for the first 6.25 years of operation from 4th August 2008 to 28th November 2014 (Mission Elapsed Time: 239557417 to 438847466) and selected events with energies >100 GeV for both front and back converting SOURCE class events. We also excluded the Galactic plane ($| b | < 10°$) from our scan as the source confusion resulting from the poor angular resolution prevents us from reliably picking out individual clusters. The data was then processed according to the pass 7 rep criteria (see full paper for more detail [1]).

For our clustering parameters, we chose a range between 0.1° to 0.5° based on the 68% and 95% containment radii for both front and back converting events above 100 GeV. As we are considering relatively low statistics, we chose *MinPts* to be the minimum number of events that could constitute a cluster statistically, namely 3 events.

For each cluster, the effective radius from the cluster centroid was calculated as $r_{eff} = \sqrt{\sigma_x^2 + \sigma_y^2}$, where σ_x and σ_y are the uncertainties expressed as the standard deviations in the event position. To

determine the significance of the cluster we applied the Likelihood Ratio Test (LRT) as described in [12] and applied in both [15] and [9],

$$s = \sqrt{2\left(N_s \ln\left[\frac{2N_s}{N_s+N_b}\right] + N_b \ln\left[\frac{2N_b}{N_s+N_b}\right]\right)} \tag{2.1}$$

where N_s is the number of events taken from the DBSCAN and includes core and border events. The background N_b was estimated from the number of events between 2 r_{eff} and 3 r_{eff}. We set a cluster significance of $s = 2$ as our minimum significance for a cluster. When N_s and N_b are large, which is not the case here, this represents a fluctuation of 2σ above the background. Therefore we use the LRT only as an indicator and in Section 4 we discuss the validity of this assumption.

A study of the effects of changing *EPS*, described in detail in the full paper [1], has shown the optimal value to be 0.4°. The results from the cluster analysis for sources with an LRT significance of $s > 2$ using an *EPS* of 0.4° can be found in Table 1, where we lists the 28 sources that are not currently part of the TeVCat[2] VHE catalogue[3] .

3. Verification of VHE Clusters using *Fermi* Analysis

For each significant cluster found using the DBSCAN algorithm, we used the full 6.25 years worth of the *Fermi*-LAT data within a ROI of radius 5° surrounding the cluster position for further analysis. As before, the data were reduced with the *Fermi* tools gtselect and gtmktime in order to apply a zenith cut and to keep only the "good time intervals" according the same pass 7 criteria for SOURCE class events between 100 and 300 GeV.

We ran an unbinned likelihood analysis on each source, modelling each cluster with a power law spectral shape of the form $dN/dE = A \times (E/E_o)^{-\Gamma}$, where A is the normalisation, Γ the spectral index and E_o the scaling factor. For each analysis we also included all point sources within 15 degrees of the cluster position, as well as the most recent Galactic (gll_iem_v06_rev1.fit), extra-galactic diffuse (iso_source_v05.txt) and extended source models in the case where such a source was found in the ROI. The position and the spectral shape of these point sources were taken from 3FGL [11]. During the analysis, the normalisation and the spectral index of the cluster source and the point sources within the ROI where left free to vary. Modelled sources outside the ROI but within 15° had their parameters frozen to those published in the 3FGL. Likewise, the normalisation factor of the extragalactic diffuse emission was left free to vary, and the Galactic diffuse template was multiplied by a power law in energy, the normalisation of which was left free to vary[4].

From the unbinned analysis with the above model, we arrived at a best-fit power law model and integrated flux for each cluster along with resulting likelihood Test Statistic (TS)[5]. If the analysis returned an insignificant result (TS <25) for the $E_\gamma \geqslant 100$ GeV flux, upper limits were calculated.

[2]Online catalogue of VHE ground based detections http://tevcat.uchicago.edu/

[3]A table of 21 detected TeVCat sources can be found in the full version of this paper [1]

[4]http://fermi.gsfc.nasa.gov/ssc/data/access/lat/BackgroundModels.html

[5]The Test Statistic is defined as $TS = -2\ln(L_{max,0}/L_{max,1})$, where $L_{max,0}$ is the maximum likelihood value for a model without an additional source (the 'null hypothesis') and $L_{max,1}$ is the maximum likelihood value for a model with the additional source at a specified location.

	Fermi ID	Counterpart ID	RA deg	Dec deg	z	$s_{0.4}$	TS 100-300 GeV	Flux 100-300 GeV $\times 10^{-11}$ ph cm^{-2}s^{-1}	TS 0.1-100 GeV	Flux 0.1-100 GeV $\times 10^{-9}$ ph cm^{-2}s^{-1}	Γ 0.1-100 GeV
1	3FGL J0209.4-5229	RBS 285	32.45	-52.48	-	2.04	37.08	1.56 ± 0.74	690.92	7.56 ± 1.00	1.74 ± 0.053
2	3FGL J0543.9-5531	RBS 0679†	85.99	-55.55	0.273	2.35	51.12	2.07 ± 0.96	722.77	8.16 ± 1.06	1.72 ± 0.051
3	3FGL J0912.9-2104	MRC 0910-208	138.31	-21.09	0.198	2.35	36.09	2.34 ± 1.09	278.69	6.25 ± 1.47	1.83 ± 0.085
4	3FGL J1031.2+5053	RBS 877	157.74	50.88	0.360	2.04	27.97	1.59 ± 0.89	465.99	5.39 ± 0.030	1.77 ± 0.0024
5	3FGL J1117.0+2014	RBS 0958	169.24	20.25	0.138	2.04	36.21	1.94 ± 1.11	802.22	14.39 ± 0.38	1.95 ± 0.010
6	3FGL J1120.8+4212	RBS 0970†	170.16	42.26	0.390	2.35	34.34	2.18 ± 1.13	730.57	4.31 ± 0.53	1.55 ± 0.050
7	3FGL J2322.5+3436	TXS 2320+343	350.63	34.60	0.098	2.35	41.82	2.13 ± 1.08	76.50	2.12 ± 0.17	1.77 ± 0.025
8	3FGL J2356.0+4037	GB6 B2353+4020	359.17	40.66	0.331	2.04	27.69	1.55 ± 0.91	91.68	2.04 ± 0.23	1.72 ± 0.040
9	3FGL J1714.1-2029	1RXS J171405.2-202747	258.48	-20.41	-	2.35	27.34	2.01 ± 1.11	43.06	1.13 ± 0.88	1.59 ± 0.23
10	Unkn. J2132.43-3416	-	323.21	-34.24	-	2.04	25.63	2.45 ± 1.84	3.83	<0.42	-
11	3FGL J2209.8-0450	-	332.44	-4.86	-	2.04	25.59	2.60 ± 1.40	27.39	1.37 ± 0.032	1.80 ± 0.0078
1	3FGL J0730.5-6606	PMN J0730-6602	112.80	-66.00	0.106	2.04	19.17	<2.10	102.93	2.59 ± 0.96	1.71 ± 0.13
2	3FGL J1309.3+4304	B3 1307+433	197.21	42.83	0.690	2.04	20.10	<1.14	1123.02	15.25 ± 0.23	1.92 ± 0.0067
3	3FGL J1659.0-0142	-	255.23	-1.44	-	2.04	15.39	<0.86	86.66	10.44 ± 3.79	2.16 ± 0.13
4	2FGL J1721.5-0718c	-	260.18	-7.20	-	2.04	12.95	<4.81	5.17	<13.2	-
5	3FGL J1838.8+4802	GB6 J1838+4802	279.68	48.01	0.300	2.04	13.57	<0.91	828.92	10.23 ± 1.06	1.79 ± 0.041
6	Unkn. J0255.43+3334	-	43.90	33.57	-	2.04	16.53	<1.20	∼0	<0.068	-
7	Unkn. J0808.43+1645	-	122.19	16.75	-	2.04	18.34	<5.08	0.03	<2.16	-
8	Unkn. J1359.3-4019	-	209.86	-40.32	-	2.04	22.44	<1.56	0.68	<21.3	-
8	Unkn. J1526.16-0515	-	231.57	-5.26	-	2.04	12.36	<1.01	∼0	<0.070	-
10	Unkn. J1626.7-0617	-	246.73	-6.29	-	2.04	23.45	<1.69	∼0	<0.011	-
11	Unkn. J1655.52+0052	-	253.99	-0.88	-	2.04	14.19	<1.22	35.37	18.90 ± 0.042	2.76 ± 0.00039
12	Unkn. J1902.14+4557	-	285.41	46.06	-	2.04	15.53	<2.24	0.67	<0.47	-
13	Unkn. J1903.33+3649	-	285.90	36.82	-	2.04	10.47	<1.26	7.13	<63.0	-
14	Unkn. J1907.07-2930	-	286.69	-29.36	-	2.04	10.34	<0.49	1.82	<10.9	-
15	Unkn. J1938.09-0350	-	294.55	-3.84	-	2.04	12.35	<1.51	1.20	<25.9	-
16	Unkn. J2001.5+0330	-	300.47	3.68	-	2.04	16.44	<1.04	∼0	<0.065	-
17	Unkn. J2212.19+8221	-	333.08	82.36	-	2.04	20.43	<1.12	∼0	<0.056	-

Table 1: Results for sources detected at E $\geqslant$ 100 GeV with DBSCAN. 'Unkn.' refers to sources that are not present in the 3FGL, z is the redshift of known counterparts, $s_{0.4}$ is the significance returned by the likelihood ratio test (eqn. 2.1. The Test Statistic (TS), flux and Γ were found with follow-up analysis using the published *Fermi* tools. The first 11 sources are those that were found to be significant (TS >25) with the the follow-up analysis. For sources with TS <25, upper limits were calculated for the flux. A binned likelihood analysis has also been applied to the energy range 0.1 >E >100 GeV in order to obtain a power-law spectral index. † previously detected in [6] and [7]

Lastly, after accounting for all point sources within the field of view with the *Fermi* tool gttsmap, one final refinement of the model file was performed, namely, the *Fermi* tool gtfindsrc which was used to determine a more precise localisation of the source's RA and Declination. The differences between the gtfindsrc results and the position found by DBSCAN all agree within the 95% PSF and in most cases to better than 0.1°. The resulting positions, fluxes and TS values of all 28 DBSCAN clusters can be found in Table 1.

4. Discussion

Using DBSCAN parameters *EPS* = 0.4° and *MinPts* = 3 on 6.25 years of *Fermi*-LAT data for $E_\gamma \geqslant 100$ GeV, excluding data from $|b| < 10°$, we have found 49 sources which return a significant likelihood ratio. Of the 61 extragalactic objects already existing in both the *Fermi*-LAT third point source catalogue (3FGL) and the TeVCat VHE catalogue, 21 are also detected using DBSCAN. Of the remaining 28, 11 were found significant with follow up *Fermi* analysis (Table 1); 10 of these are in the 3FGL catalogue, which reports fluxes only up to 100 GeV.

DBSCAN Performance: To estimate the performance of the DBSCAN algorithm in the case of VHE detections, we define the concept of *purity* as the number of sources with TS>25 (including the sources already in the TeVCat catalogue) against the total found by the DBSCAN clustering code. In the full version of this paper [1], we show that in order to maximise the number of sources

with TS >25 detected, with the maximum purity, an *EPS* of 0.4° should be used by DBSCAN. Therefore we present our results for this value.

To investigate the performance of the likelihood ratio test (LRT) significance, s, in equation 2.1, the LRT values for the clusters were compared to the TS values obtained with the *Fermi* Likelihood analysis. In Figure 1, the LRT vs TS parameter space shows a clear correlation, with a large amount of quantisation of the LRT distribution for low s values. This quantisation is primarily due to the lack of background events detected with the LAT detector in $E_\gamma > 100$ GeV energy regime. While this suggests that the use of the LRT to define a DBSCAN cluster as significant results in a large number of false-positive detections, we note that our use of a LRT selection criteria of $s > 2.0$ is a conservative cut so as to guarantee the selection of all VHE sources in our sample. As such, while our use of $s > 2.0$ is sub-optimal for selecting VHE candidates with a high purity, Figure 1 shows that this allows us to find all VHE sources present within our data set and thus maximises the number of new sources discovered. Nonetheless, further work should be performed in order to investigate viable alternatives to the LRT that simultaneously maximises both the VHE-detection efficiency **and** the sample purity.

A full understanding of the efficiency of DBSCAN in this application is somewhat more complex, requiring detailed simulations and modelling of the *Fermi* VHE sky, which goes beyond the scope of this paper. However, estimations of DBSCAN efficiency can be found in [15] where, by simulating a range of false sky maps, they find it possible to achieve efficiencies of up to 96%. This must be treated as an optimistic scenario as it is based on an optimal scan of the *EPS-MinPts* parameter space. We expect the efficiency to be much lower in our case due to our assumption of minimal background variation, which will be addressed in future work.

Although we note that there are still improvements to be made with the DBSCAN method, we draw attention to its capability of performing an quick, unbiased scan for potential “seed" sources in the VHE *Fermi*-LAT sky which in this study has led to the detection of 9 new VHE sources.

Detected VHE Sources: To investigate the global properties of the *Fermi*-LAT VHE sources detected by the DBSCAN algorithm, we ran a binned likelihood analysis over the energy range 100 MeV to 100 GeV in order to to obtain a reliable model file with higher statistics. The data reduction method follows as previously, but this time using a ROI of 12° centred on the published location of the source, keeping all modeled source parameters within this ROI free and freezing sources within an annulus 12° to 22° from the source of interest. For the analysis, the data were separated into 30 equally-spaced logarithmic energy bins. The resulting fluxes, spectral indices and TS values of the likelihood fits for these objects can be found in Table 1. For sources with TS <25, upper limits where calculated from the final fit and no spectral index is quoted.

Out of the 11 sources detected, we note that 9 of them are blazars and all, except for 3FGL J1714.1-2029 which is of unknown AGN type, belong to the BL Lac class. The remaining 2 do not have any assigned counterparts. For each source we looked for temporal clustering of the VHE events but found no evidence to suggest that the VHE photons originated in a single event.

The source of unknown type, 3FGL J2209.8-0450, which is a new addition since the 2FGL, is only 54.55” away from the radio source NVSS J220941-045111 (which is also connected to the X-ray object 1RXS J220942.1-045120). The second unassociated source has no known counterpart in the 3FGL and no clear radio association, however its position is coincident with the galaxy group ESO 403-6. Although this source was detected in the 100 GeV to 300 GeV range with a flux of

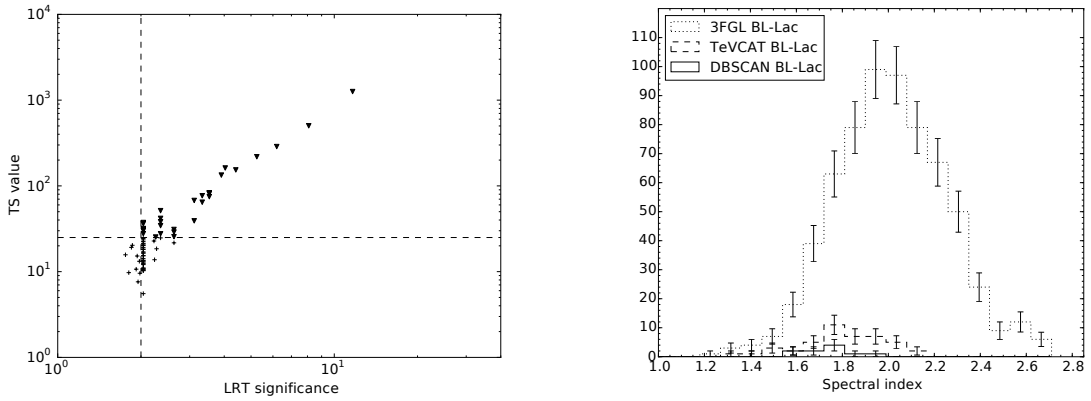

a) b)

Figure 1: (a) Comparing the value of LRT and TS for each cluster, we can see the quantisation of the LRT due to a breakdown in the assumption that the number of signal and background events are not too small is clear. The solid triangles indicate the clusters with TS$>$ 25, while the crosses indicate the clusters with TS$<$ 25. The vertical dashed line indicates our LRT cut value, while the horizontal dashed line indicates our TS$>$ 25 cut value.(b) Histogram showing the spectral index distribution of the 3FGL and TeVCat BL Lac populations compared to those found in this work. Performing a standard independent 2-sample t test infers that the 11 significant sources in Table 1 come from the same distribution as the VHE TeVCat sources.

$(2.45 \pm 1.84)\times10^{-11}$ ph cm^{-2}s^{-1} it appears to have no significant emission in the energy range of 100 MeV to 100 GeV, making this an interesting VHE dark source. More work needs to be carried out in order to correctly identify counterparts for these sources.

In order to determine the likelihood that any of the unassociated sources with TS <25 are unresolved AGN, we checked for any coincidence with BZCAT sources [13]. We find no evidence of any association within the 95% PSF, suggesting that a large proportion of these clusters arise from fluctuations in the background or from a larger unresolved structure.

We then compared the spectral index distribution of the sources found using DBSCAN with the total 3FGL BL Lac population and those which are also in the TeVCat catalogue. The result of this comparison is shown in Figure 1. In order to test whether the different distributions have the same mean and variance, we performed a standard independent 2-sample t test on the DBSCAN sample and each of the spectral index distributions. Having initially set a significance level of 5%, we find that the *Fermi* VHE sources detected with DBSCAN are better represented by the TeVCat BL Lacs, with a P value of 0.368, than the total 3FGL BL Lacs for which we obtain a P value of 0.000547.

We suggest that the sources we have detected with VHE emission, provided there are no spectral cut-offs, should be within reach of current and future ground based Imaging Atmospheric Cherenkov Telescopes (IACTs) and should undergo follow up observations.

5. Conclusions

We have presented an application of the clustering algorithm DBSCAN to 6.25 years of *Fermi*-LAT extragalactic data above 100 GeV, finding 49 clusters which were found significant using a likelihood ratio test. Of the 28 which are not already known in the TeVCat ground-based catalogue,

we found 11 that were significant (TS>25) with follow up *Fermi* likelihood analysis. With the 2 sources RBS 0679 and RBS 0970 having previously been detected at E $\geqslant$ 100 GeV [6, 7], we therefore present 9 new VHE objects consisting of 7 AGN and 2 unassociated sources.

We have performed a preliminary analysis into some of the global properties of these new *Fermi* VHE sources. Concerning the spectral indices derived from a fit between 100 MeV and 100 GeV, we see that these sources are more similar to the the TeVCat BL Lac sources than to the overall 3FGL BL Lac population. We take this as a strong indication that these should be observable by current and future ground based IACTs. A full analysis and description of these sources will be presented in future work.

Acknowledgment:TPA would like to acknowledge the support of a studentship from the UK Science and Technology Facilities Council grant ST/K501979/1. AMB would like to acknowledge the financial support of Durham University. This work has made use of publicly available *Fermi*-LAT data from the High Energy Astrophysics Science Archive Research Center (HEASARC), provided by NASAs Goddard Space Flight Center.

References

[1] T. Armstrong, A. M. Brown, P. M. Chadwick and S. J. Nolan. *The Detection of Fermi AGN above 100 GeV using Clustering Analysis* [astro-ph/1506.06947]

[2] Abdo, A. A., Ackermann, M., Ajello, M., et al. *The Spectrum of the Isotropic Diffuse Gamma-Ray Emission Derived From First-Year Fermi Large Area Telescope Data* 2010 *PRL* **104**, 10, 101101, [astro-ph/1002.3603]

[3] Ackermann, M., Ajello, M., Albert, A., et al. *The Fermi Large Area Telescope On Orbit: Event Classification, Instrument Response Functions, and Calibration*, 2012, *APJs*, **203**, 4 [astro-ph/1206.1896]

[4] Actis, M., Agnetta, G., Aharonian, F., Akhperjanian, A., Aleksic, J. et al., *Design Concepts for the Cherenkov Telescope Array*, 2011, *Exp. Astron.*, **32**, 193 [astro-ph/1008.3703]

[5] Atwood, W.B. et al., *The Large Area Telescope on the Fermi Gamma-ray Space Telescope Mission*, 2009, *ApJ*, **697**, 1071, [astro-ph/0902.1089]

[6] Brown A.M., *Very High Energy gamma-ray emission from RBS 0970*, 2014, *MNRAS*, **442**, L56-L60 [astro-ph/1404.3586]

[7] Brown A.M., Chadwick P.M., Landt, H., *Very high energy γ-ray emission from RBS 0679* 2014, *MNRAS*, **445**, 4345-4350, [astro-ph/1410.1709]

[8] Campana, R., Massaro, E., Gasparrini, D., Cutini, S., & Tramacere, A., *Minimal spanning tree algorithm for Îş-ray source detection in sparse photon images: cluster parameters and selection strategies*, 2008, /emphMNRAS, **383**, 1166 [astro-ph/1305.2025]

[9] Carlson E., Linden T., Profumo S., and Weniger C., *A Clustering Analysis of the Morphology of the 130 GeV Gamma-Ray Feature*, 2013, *Physical Review D*, **88**, 043006, [astro-ph/1304.5524]

[10] Ester M., Kriegel H.P., Sander J., and Xu X., *A Density-Based Algorithm for Discovering Clusters in Large Spacial Databases with Noise*, 1996, *AAAI Press*, pp. 226-231.

[11] The Fermi-LAT Collaboration, *Fermi Large Area Telescope Third Source Catalog*, 2015, [astro-ph/1501.02003]

[12] Li, T. P. and Ma, T. Q., *Analysis Methods for Results in Gamma-Ray Astronomy*, 1983, *Astrophysical Journal*, **272**, 317

[13] Massaro, E., Giommi, P., Leto, C., et al. *Roma-BZCAT: A multifrequency catalogue of Blazars*, 2009, *AAP*, **495**, 691 [astro-ph/0810.2206]

[14] Sol, H., Zech, A., Boisson, C., et al. *Active Galactic Nuclei under the scrutiny of CTA*, 2013, *Astroparticle Physics*, **43**, 215 [astro-ph/1304.3024]

[15] Tramacere A., and Vecchio C., *Gamma-Ray DBSCAN: A Clustering Algorithm Applied to Fermi-LAT Gamma-Ray dData. I. Detection Performances with Real and Simulated Data*, 2013, *A&A*, **549**, A138, [astro-ph/1210.0522]